Dicle University
Journal of Engineering
https://dergipark.org.tr/tr/pub/dumf
duje.dicle.edu.tr

Research Article

Boriding Effect on the Hardness of AISI 1020, AISI 1060, AISI 4140 Steels and Application of Artificial Neural Network for Prediction of Borided Layer

Mehmet ÖZER[1], Fatih BALIKOĞLU[2], Tayfur Kerem DEMİRCİOĞLU[3*], Yunus Emre NEHRİ[4]

[1] Balıkesir University, Department of Transportation Services, ozer@balikesir.edu.tr, Orcid No: 0000-0002-6212-1217
[2] Balıkesir University, Mechanical Engineering Department, fatih@balikesir.edu.tr, Orcid No: 0000-0003-3836-5569
[3] Balıkesir University, Mechanical Engineering Department, tkerem@balikesir.edu.tr, Orcid No: 0000-0002-0518-0739
[4] Balıkesir University, Mechanical Engineering Department, yunusnehri@balikesir.edu.tr, Orcid No: 0000-0003-2119-9031

ARTICLE INFO

Article history:

Received 11 November 2023
Received in revised form 23 February 2024
Accepted 4 March 2024
Available online 29 March 2024

Keywords:

artificial neural network, boronizing, borides

ABSTRACT

Artificial neural network approach was used to predict the thicknesses of total (FeB+Fe_2B), FeB and Fe_2B borides layers of AISI 1020, AISI 1060, and AISI 4140 steels. Boronizing heat treatment was conducted in a solid medium comprising of EKabor®2 powders at 840–960 ˚C at 40 ˚C intervals for 2, 4, 6, and 8 hours. Optical microscope analysis of the borided layer revealed the saw-tooth (columnar) and planar morphology. The depth of the total (FeB+Fe_2B), FeB and Fe_2B boride layers was accurately predicted. For total boride layers generated by the artificial neural network model, the average error varied between 0.04 and 7.64 µm. Micro hardness values increased by 423% in AISI 1020, 336% in AISI 1060, and 411% in AISI 4140 after the boronizing process.

Doi: 10.24012/dumf.1389301

* Corresponding author

Introduction

The need to improve surface properties such as corrosion resistance, wear resistance, oxidation resistance and friction has led to the development of numerous surface improvement methods, which are decisive in increasing the service life of many engineering components [1]. Boronizing, which is one of them, is a thermochemical process in which boron atoms diffuse from the surface of the steel alloys towards the interior. Generally, boronizing process is applied in range of 700 ºC – 1050 ºC and 0.5 to 10 hours. Boronizing is applied to improve the surface properties of steels such as corrosion and wear resistance [2]. Boriding process can be carried out in solid, liquid, or gaseous medium. The most widely used boriding method is the pack method, which has the advantages of ease of application and low cost [3, 4].

Boriding produces single-phase (Fe_2B) or dual-phase (FeB + Fe_2B) iron boride surface compounds. Depending on the concentration of the diffused boron atoms, the boride layer may consist of tetragonal Fe_2B (8 wt % B) and/or orthorhombic FeB (16 wt % B) [5]. In general, the FeB phase, which has a lower toughness than the Fe_2B phase, is characterized by a higher hardness [6, 7]. The presence of a dual-phase layer (FeB + Fe_2B) is undesirable for industrial applications because each phase has very different properties such as coefficient of thermal expansion (CTE) and elastic modulus; The CTE of FeB and Fe_2B are 23 and $8 \times 10{-}6$ ºC^{-1}, respectively, while Young's modulus is 510 GPa and 280 GPa, respectively. Such differences in properties can generate high compressive residual stresses at the interface (FeB + Fe_2B) during the formation of the layers. It can lead to the formation and propagation of cracks at the interface of the two phases [8, 9]. Furthermore, the FeB phase is undesirable in the boride layer due to its higher brittleness, which induces shedding from the surface when subjected to strong external loads [10, 11].

Boronizing process can be applied to many materials such as surface hardened steels, annealed steels, tool steels, stainless steels, cast irons, sintered metal powders, nickel, cobalt, molybdenum, titanium, non-ferrous metals and their alloys, and some super alloys and cermet [9, 12]. The most significant characteristics of boride phases generated by boriding are high hardness (1400-5000 HV) and high melting temperature (1400-1550 ºC) [13, 14]. Boriding is a surface hardening method that can obtain the hardest layer on the surface compared to other methods [15, 16]. It is well known that the fatigue life of boronized industrial metals increases as surface hardness increases [17, 18]. The boron

layer thickness, which generally occurs in low carbon unalloyed steels, is up to 0.4 mm. The increased amount of carbon or the presence of the alloying element (Cr, V and others) causes the layer thickness to decrease [19, 20]. Besides, a high amount of chromium (for example) encourages the formation of FeB rather than Fe_2B. Kul, M., et al. [21] applied surface hardening process to the camshafts made of AISI-1045 steel by boronizing in liquid and solid media. To obtain the hardest and thickest boride layer in the samples, the proposed composition in the liquid medium was 70% Borax ($Na_2B_4O_7$) + 30% B_4C. Furthermore, the results indicated that a suitable composition for solid media boriding is 5% B_4C + 90% SiC + 5% KBF_4. Joshi, A. A., et al. used the package boriding process for small, medium, and large sized containers made of AISI 4140 steel for 2 and 3 hours at 950 ºC. The results showed that the morphology of the Fe_2B phase was columnar, and the hardness decreased from the surface towards the inner part. A maximum surface hardness of about 1367 $HV_{0.1}$ was obtained for boronized steel [22]. Şahin, S. applied the solid boriding process on AISI 1020, AISI 1040 and AISI 2714 steels at 900 ºC in 2 and 4 hours using Ekabor I powder. It was observed that the dimensional increase of the samples was one-fifth of the boride layer thickness for both AISI 1020 and AISI 1040, and one-third of the boride layer thickness for AISI 2714. The authors proposed the term "threshold roughness", which corresponds to the surface roughness value for boron-treated smooth surfaces [23].

This study evaluates the enhancements in boron diffusion depths and hardness values of AISI 1020, AISI 1060, and AISI 4140 steel specimens obtained using the pack boriding process. The effect of temperature and time parameters in boriding process was investigated. With the artificial neural network (ANN) application, the prediction was made for the total, FeB and Fe_2B boride layer thicknesses.

Materials and Method

Materials

Pack boriding process was applied for low carbon AISI 1020, high carbon AISI 1060 and alloy AISI 4140 steel materials. The contents of the AISI 1020, AISI 1060 and AISI 4140 steel specimens are given in Table 1. The cylindrical test specimens with a diameter of 15 mm and a height of 20 mm were used.

Application of Boronizing Process

Three replicates were prepared for different temperature and time parameters to determine the effect of boronizing on the surface hardness of AISI 1020, AISI 1060 and AISI 4140 steels. For comparison, one sample of each specimen was subjected to the necessary measurements without boronizing. Boronizing test parameters and specimen codes are shown in Table 2. Boronizing process was carried out under these conditions.

Boronizing heat treatment was performed in a solid state. For each test condition, 9 samples were placed in the stainless-steel box and heated in the furnace. The test period begins when the furnace reaches the desired temperature. Boron powder, " EKabor®2" is used as a boron supplying compound in the form of B_4C - SiC - KBF_4. The particle size of the powders is (75 - 106 μm). After filling the stainless-steel box with 2 cm of EKabor®2powder, the specimens are placed at least 1 cm apart from the sides and from each other. The specimens were then filled with 2 cm EKabor®2 powder, Ekrit® powder was added as deoxidant on the top, and the cover was closed. Ekrit® consists of pure iron and oxide scavenger components. All samples were subjected to boronization process using this method at different temperatures and times. Following the boronizing heat treatment, the specimens were removed from the box and cleaned after cooling.

Metallographic Examination

Boronized specimens with dimensions of Ø 15 × 20 mm were cut into half along the radius axis using a precision cutting instrument and prepared for metallographic examinations.

Specimens with rectangular cross-sections were grinded with sandpaper numbers 180, 220, 320, 400, 600, 800, 1000, 1200, respectively, at a speed of 200 rpm in the "Buehler-Metaserv" grinder/polisher device. After that in the same device, they were polished on the broadcloth with 6 μm and 1 μm diamond polishers. The polished specimens were etched with 4% Nital (Nital: HNO_3+Ethyl Alcohol) solution for 10 seconds.

The microstructure photographs of the specimens prepared for metallographic examination were taken with a Nikon MA 100 optical microscope. The FeB phase close to the surface and the Fe_2B phase below this phase can be distinguished due to the color difference obtained by etching. The depth of the boride layer formed on the cross-sectional surfaces of the samples was measured with the same optical microscope and marked on photographs.

Hardness Measurement

The hardness distributions of the coating and matrix were measured with the Shimadzu micro hardness device. Hardness tests were carried out using a Micro-Vickers tip with 50 g load and 10 sec. Hardness measurements were conducted inward from the surface of all samples were carried out in the range of 20 – 50 μm. A wider range was made in the samples with a greater diffusion depth, and a narrower range was made in the samples with a low diffusion depth.

Table 1. The chemical compositions of the AISI 1020, AISI 1060 and AISI 4140 steels.

Materials	C%	Si%	Mn%	P<	S<	Cr	Mo	Ni
AISI 1020	0.38-0.45	0.15-0.40	0.50-0.80	0.035	0.035	0.90-1.20	0.15-0.30	-
AISI 1060	0.18-0.25	0.15-0.35	0.30-0.60	0.035	0.035	-	-	-
AISI 4140	0.55-0.64	0.10-0.30	0.60-0.90	0.040	0.050	-	-	-

The measurement was taken at regular intervals from the surface to the matrix, and the arithmetic average of at least five replicates was calculated. It was observed that the hardness values of the formed boron layer measured inward from the surface are compatible with the literature [22, 24, 25]

Artificial Neural Networks Simulation Model

Artificial neural networks (ANN) are a computational model inspired by neurons in the human brain and the connections between them [26]. Neural networks are well-known as a very general statistical framework for predicting sample data from a set of data [27].

Artificial neural networks enable the creation of a computational model inspired by the biological neural network structure, using neurons for computation. In the artificial neural network system, there are three layers: input, hidden, and output. The input layer represents the independent variables and transmits these variables to the hidden layer with certain weight coefficients. The processed information in the hidden layer is then sent to the output layer for computation. The output layer represents the dependent variable obtained based on the independent variables from the input layer. The network used in this study is presented in Figure 7. In this study, steel type, time, and temperature are taken as independent variables. The dependent variables are the boron layer thickness affected by these independent variables (Fe_2B+FeB), Fe_2B thickness, and FeB phase. In the experimental results, 64 data (80% of test data) were used to train the artificial neural network, and the remaining 16 data (20% of test data) were used to train the artificial neural network. The TRAINLM algorithm is used in the training of artificial neural networks because it is fast and has high memory. As the structure of the network, a more reliable "feed-forward backprop", which proceeds with the control of errors, was chosen. The LEARNGDM learning function and the TANSIG transfer function are used for network learning. Training was carried out using 12 hidden neurons in 3 layers. As seen in Figure 7, there are five different parameters as independent variables. Five different input parameters as three different steel specimens, temperature, and time were taken into consideration.

Results and Discussion

Hardness and Microstructure Analysis

AISI 1020 Steel

Figure 1 a, b, c shows the dual-phase (FeB + Fe_2B) layers of boronized AISI 1020 steel at 840, 880 and 920 ºC for 8 hours, respectively. The Fe_2B layer was isolated with the FeB teeth for the AISI 1020 specimens, which boronized for 8 hours. The thickness of the FeB layer on the surface increased with increasing temperature up to 920 ºC. Diffusion depths of the AISI 1020 steel boronized at 840, 880, 920 and 960 ºC for 8 hours were 116 µm (± 2 µm), 119 µm (± 5 µm), 199 µm (± 5 µm), 211 µm (± 8 µm), respectively. Figure 1 d, e shows the single-phase Fe_2B layer of AISI 1020 steel boronized at 960 ºC for 2 and 4 hours, respectively. By doubling the heat treatment time, the Fe_2B phase became more prominent as it was very isolated; the Fe_2B layer thickness increased and showed saw-tooth structures. Diffusion depth of AISI 1020 steel boronized at 960 ºC for 2 and 4 hours, respectively, increased from 24 µm (± 1 µm) to 64 µm (± 3 µm), respectively. The dual-phase structure was observed as a result of applying heat for 6 and 8 hours at 960 ºC (Fig. 1 f, g). Diffusion depths resulting from boronizing at 960 ºC for 6 and 8 hours were measured as 141 µm (± 7 µm) and 211 µm (± 8 µm), respectively. Figure 4 shows the variation of boron diffusion depth of AISI 1020 steels with temperature and time. The results showed that a deeper diffusion layer was formed in each time period of 960 ºC compared to other temperature conditions. In comparison to AISI 1060 steel and AISI 4140 steel, AISI 1020 steels tend to exhibit a high micro hardness throughout deeper distances. Since the boriding morphology for AISI 1020 had discontinuous saw-tooth structures, the measured hardness values varied depending on the testing area compared to other samples. In AISI 1020 steels, the increase in hardness values depending on the temperature for the 8-hour boriding time was lower compared to the AISI 1060 and AISI 4140 samples (Fig 5a-c).

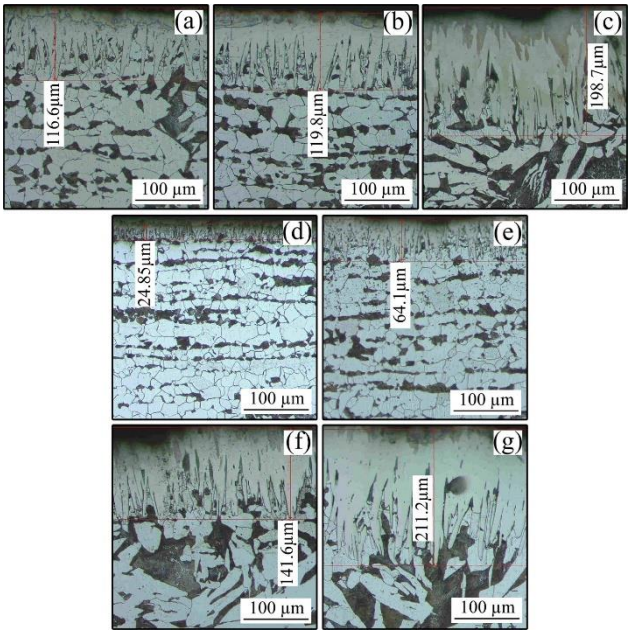

Figure 1. Microstructure images of AISI 1020 steel

AISI 1060 Steel

Figure 2 a, b, c shows the dual-phase (FeB+ Fe_2B) layer of AISI 1060 boronized steel at 840, 880 and 920 ºC for 8 hours. The diffusion depth of AISI 1060 boronized steel at 840, 880 and 920 ºC for 8 hours was measured as 100 µm (± 2 µm), 124 µm (± 3 µm) and 188 µm (± 5 µm), respectively. Figure 2 d, e shows the single phase Fe_2B layer of AISI 1060 boronized steel at 960 ºC for 2 and 4 hours, respectively. The diffusion depth of AISI 1060 boronized steel at 960 ºC for 2 and 4 hours increased from 22 µm (± 1 µm) to 58 µm (± 2 µm), respectively. The dual-phase structure was observed as a result of 6 and 8 hours of heat

treatment at 960 ºC (Fig. 2 f, g). The diffusion depths as a result of the boronization at 960 ºC for 6 and 8 hours was measured as 162 µm (± 4 µm) and 204 µm (± 6 µm), respectively. The fluctuation of boron diffusion depth as a function of temperature and time in AISI 1020 steels is summarized in Figure 4. The saw-tooth morphology was located more frequently since AISI 1060 steels contain more carbon than AISI 1020 steel. For AISI 1060 steels, as seen in Figure 5b, the hardness increase trend in the Fe_2B and FeB layers is more noticeable.

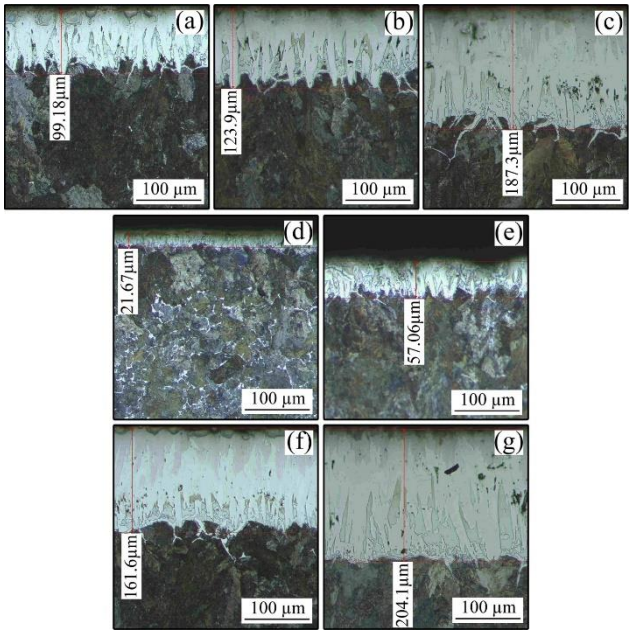

Figure 2. Microstructure images of AISI 1060 steel

AISI 4140 Steel

Figure 3 a, b, c shows the dual-phase (FeB + Fe_2B) layers of boronized AISI 4140 steel at 840, 880, 920 and 960 ºC. The diffusion depth of AISI 4140 boronized steel at 840, 880, 920 and 960 ºC for 8 hours was measured as 84 µm (± 1 µm), 114 µm (± 1 µm), 156 µm (± 2 µm) and 204 µm (± 2 µm), respectively. It was observed that Fe_2B showed a saw-tooth structure at 840, 880 and 920 ºC for 8 hours. As a result of the heat treatment at 960 ºC for 8 hours, it was seen that the Fe_2B phase had a planar structure (Fig.3 g). Figure 3 e, f shows the single phase Fe_2B layer of AISI 4140 boronized steel at 960 ºC for 2 and 4 hours. The heat treatment at 960 ºC for 6 hours produced FeB+Fe_2B dual-phase structures (Fig.3 f). Figure 4 shows the boron diffusion depth of AISI 4140 steels as a function of temperature and time. As AISI 4140 steel had a planar boron layer, the hardness test values were more uniform across the diffusion depth. The hardness value of AISI 4140 steels maintained low when compared to other materials as a result of the boriding method used with the temperature increase during an 8-hour period (Fig. 5c).

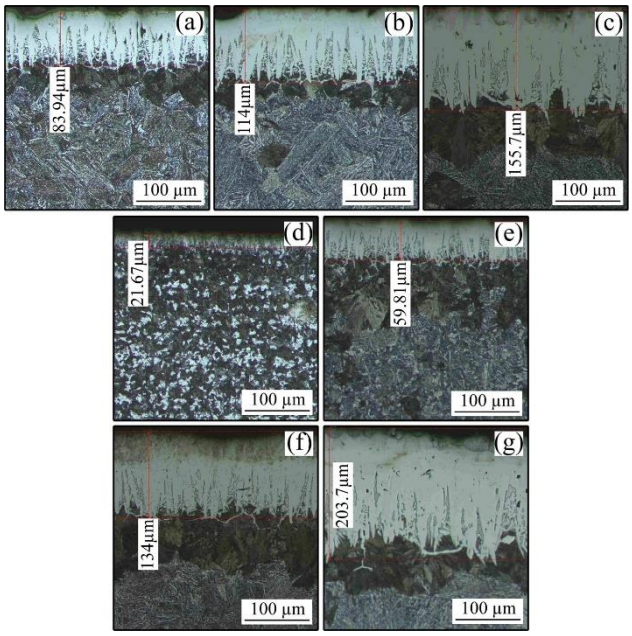

Figure 3. Microstructure images of AISI 4140 steel

Table 2. Boride layer thicknesses depending on temperature and time.

Boriding parameters		Thicknesses of boride layers		
Temperature (ºC)	Time (h)	AISI 1020 (µm)	AISI 1060 (µm)	AISI 4140 (µm)
840	2	9.15	12.86	9.33
	4	42.9	37.18	35.73
	6	79.11	57.57	60.97
	8	111.6	99.18	83.94
880	2	12.13	15.12	8.85
	4	26.11	29.39	32.62
	6	75.94	51.76	50.9
	8	119.8	123.9	114
920	2	22.35	17.3	27.17
	4	53.83	56.82	43.17
	6	110.8	106.5	102.1
	8	198.7	187.3	155.7
960	2	24.85	21.63	21.67
	4	64.1	57.06	59.81
	6	141.6	161.6	134
	8	211.2	204.1	203.7

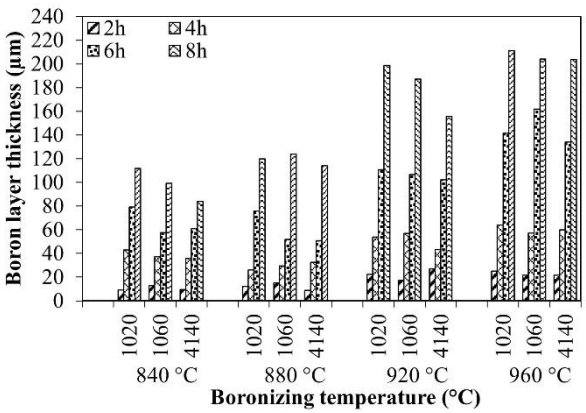

Figure 4. Boron diffusion depth as a function of on temperature and time

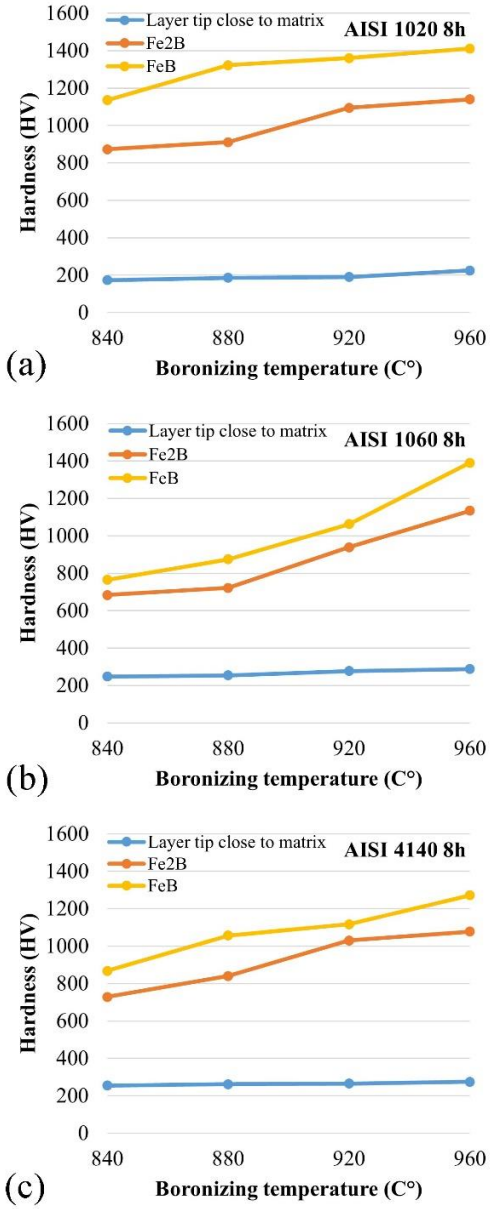

Figure 5. Hardness levels of samples as a function of temperature at 8 hours boronizing process

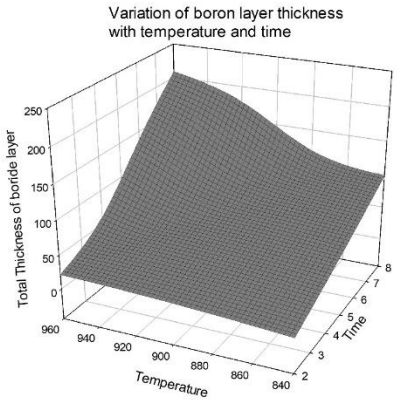

Figure 6. Variation of boron layer thickness with temperature and time

Artificial neural network approach

The purpose of using artificial neural networks in this study is to estimate the boron layer thickness by applying different temperatures on AISI 1020, AISI 1060 and AISI 4140 steels at different times**.** Table 3 provides knowledge about the ANN network. As seen in Figure 7, there are five different parameters as independent variables. Five different input parameters as three different steel specimens, temperature and time were taken into consideration. The boron layer thickness resulting from five different input parameters, the predicted values of Fe_2B and FeB, and the regression coefficients with the relationship between the measurement values are presented as seen in Table 4. The changes were made in the number of neurons, learning rates and momentum coefficients and the optimum network structure was decided.

Table 3. Networks details

Training	Levenberg-Marquardt
Network of Structure	feed-forward backprop
Learning Function	LEARNGDM
Transfer Function	TANSIG
Performance	Mean Squared Error
Calculations	MEX

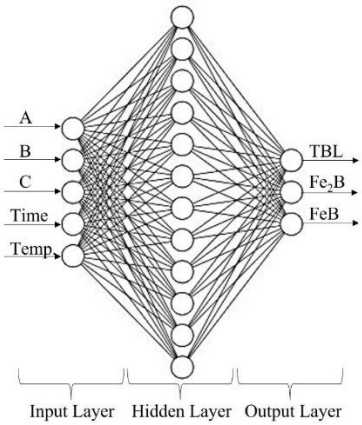

Figure 7. The structure of neural network

The actual values of the boride thicknesses measured because of the experiments and the predicted layer thicknesses given by ANN model are given in Table 4. It was observed that the predicted values approached the regression line by means of the conditional averages obtained. All experiments were performed at 95% confidence intervals. The regression coefficient (R^2 >0.99) indicated that the models constructed in the experimental analysis were relatively robust and therefore the ratios were acceptable (Figure 8). As seen in Figure 9, the model prediction shows a good agreement with experimental results. The error in the total boride layer thickness for different processing times varies between 0.04 and 7.64 µm.

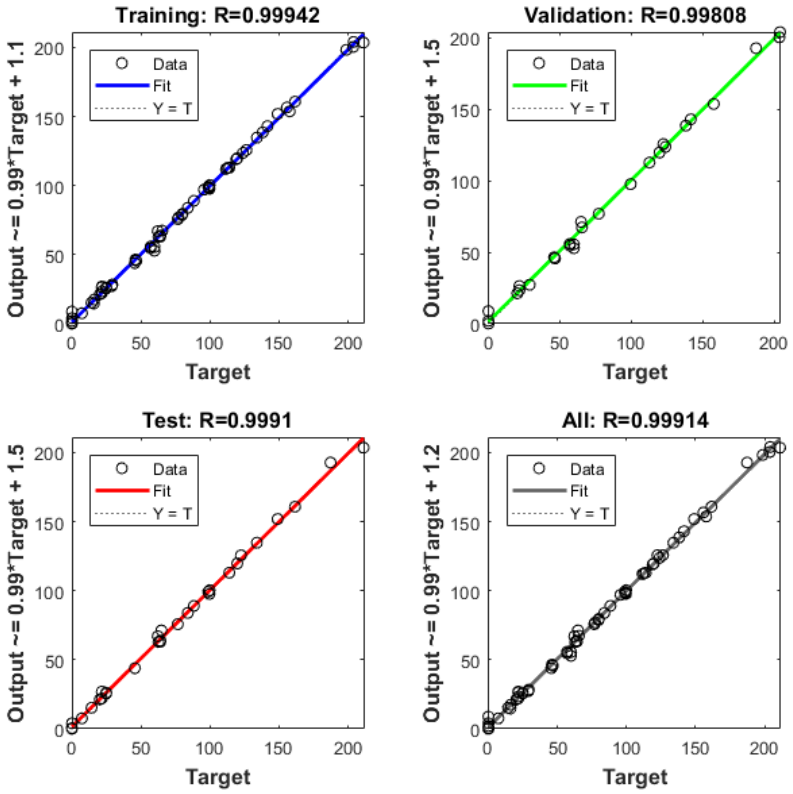

Figure 8. Regression analysis

Table 4. Actual and predicted boride layers

A	B	C	Time (h)	Temperature (°C)	Total thickness of boride layer (µm)	Predicted total thickness of boride layer (µm)	Error (µm)	Thickness of Fe_2B layer (µm)	Predicted thickness of Fe_2B layer (µm)	Error (µm)	Thickness of FeB layer (µm)	Predicted thickness of FeB layer (µm)	Error (µm)
1	0	0	4	960	59.81	55.53	4.279	59.81	52.85	6.965	0	8.83	8.832
1	0	0	6	960	134	134.73	0.735	88.38	89.05	0.668	45.61	43.91	1.701
1	0	0	8	840	83.94	83.87	0.067	76.71	75.76	0.952	7.23	7.57	0.342
1	0	0	8	880	114	113.06	0.944	99.75	100.38	0.628	14.25	15.28	1.032
1	0	0	8	920	155.7	156.61	0.906	126.42	125.78	0.644	29.27	28.39	0.883
0	1	0	2	960	21.63	21.99	0.359	21.67	26.97	5.302	0	0	0.002
0	1	0	4	960	57.06	55.88	1.175	57.06	54.68	2.382	0	2.06	2.058
0	1	0	8	840	99.18	98.5	0.683	80.01	79.6	0.408	16.17	17.46	1.287
0	1	0	8	880	123.9	123.7	0.203	77.26	77	0.259	46.64	45.64	1.002
0	1	0	8	920	187.3	192.83	5.525	122.47	125.68	3.214	64.83	71.24	6.415
0	1	0	8	960	204.1	204.06	0.043	157.7	153.78	3.917	46.03	46.52	0.485
0	0	1	4	960	64.1	63.16	0.945	64.1	63.83	0.275	0	4.02	4.02
0	0	1	6	960	141.6	143.04	1.439	112.7	112.81	0.115	28.9	27.22	1.679
0	0	1	8	840	111.6	112.05	0.447	95.7	97.02	1.319	15.9	14.63	1.271
0	0	1	8	920	198.7	198.34	0.357	119	119.09	0.092	79.7	78.7	0.997
0	0	1	8	960	211.2	203.56	7.641	149	151.92	2.916	62.2	67.07	4.866

*A=AISI 1020, B=AISI 1060, C=AISI 4140

Figure 9 illustrates a comparison of the thickness of the predicted borided layer with the experimental results. There is a considerable agreement between the experimental and predicted findings. Based on these results, it can be concluded that neural network approach has emerged as an option to model the boriding process.

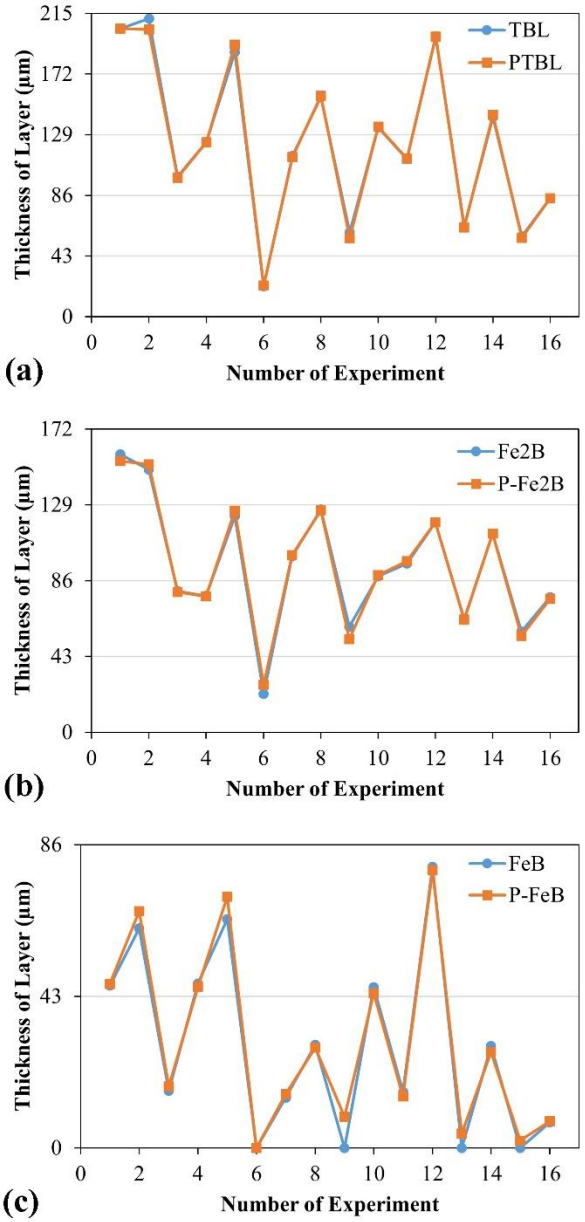

Figure 9. Comparison of predicted and experimental results of total boride (a), Fe_2B (b) and FeB (c) layer thicknesses (TBL: Total thickness of boride layer, PTBL: Predicted total thickness of boride layer, P-Fe_2B: predicted thickness of Fe_2B, P-FeB: thickness of FeB layer).

Conclusion

As expected, as the duration of the boronization process increased, the boron diffusion depth increased, and this resulted in an increase in the volume of materials. This increment should be taken into account considering sizing boronized materials.

Since the boron diffusion depth was higher in AISI 1020 steel, the dimensions increased more than the AISI1060 and AISI4140 specimens. The increase in dimensions was followed by AISI 1060 and AISI 4140 specimens.

Boron layer depth in all samples showed with increase in boronizing time. The lowest boron layer occurs at 2-hour boronizing, while the largest boron layer occurs at 8-hour boronizing.

Metallographic investigations revealed that the boride layer formed by the boron compounds in the AISI 1020 specimens has a columnar and saw-tooth structure. In the AISI 1060 specimens, on the other hand, the boron layer is formed less columnar and less toothed than the AISI 1020 specimen due to the excess of carbon. In the AISI 4140 specimen, due to the excess of alloying elements, it was observed that a boron layer with a planar geometry than the other two specimens was formed.

The findings of the neural network algorithm used to predict the thickness of the borided layer are quite acceptable for industrial applications. The ANN method produced good results in simulations for predicting boride layers. Prediction accuracy is dependent on the reliability of measured data, which should represent real correlations between temperature, time, and boride layer thickness.

In terms of micro hardness, an increase of 423% in AISI 1020, 336% in AISI 1060 and 411% in AISI 41040 was observed in the samples.

Although the order of untreated sample hardness from the hardest to the softest is AISI 1060 - AISI 4140 - AISI 1020, this order changed from hardest to softest AISI 1020 - AISI 1060 and AISI 4140 after boronization process.

Ethics committee approval and conflict of interest statement

Ethics committee approval is not required for this study.

There is no conflict of interest for this study.

Authors' Contributions

We declare that all authors equally contribute.

References

[1] T. Balusamy, T. S. Narayanan, K. Ravichandran, I. S. Park, and M. H. Lee, "Pack boronizing of AISI H11 tool steel: Role of surface mechanical attrition treatment," Vacuum, vol. 97, pp. 36-43, 2013.

[2] M. Kulka, M. Kulka, and Castro, Current trends in boriding. Springer, 2019.

[3] O. Ozdemir, M. Omar, M. Usta, S. Zeytin, C. Bindal, and A. Ucisik, "An investigation on boriding kinetics of AISI 316 stainless steel," Vacuum, vol. 83, no. 1, pp. 175-179, 2008.

[4] Y. Kayalı, "Investigation of diffusion kinetics of borided AISI P20 steel in micro-wave furnace," 2015.

[5] I. Campos-Silva, M. Ortiz-Domínguez, N. López-Perrusquia, A. Meneses-Amador, R. Escobar-Galindo, and J. Martinez-Trinidad, "Characterization of AISI 4140 borided steels," Applied Surface Science, vol. 256, no. 8, pp. 2372-2379, 2010.

[6] A. Günen, M. S. Gök, A. Erdoğan, B. Kurt, and N. Orhan, "Investigation of microabrasion wear behavior of boronized stainless steel with nanoboron powders," Tribology Transactions, vol. 56, no. 3, pp. 400-409, 2013.

[7] M. S. Gök, Y. Küçük, A. Erdoğan, M. Öge, E. Kanca, and A. Günen, "Dry sliding wear behavior of borided hot-work tool steel at elevated temperatures," Surface and Coatings Technology, vol. 328, pp. 54-62, 2017.

[8] A. I. H. Committee and A. S. f. M. H. T. Division, Heat treating. ASM international, 1991.

[9] C. Martini, G. Palombarini, G. Poli, and D. Prandstraller, "Sliding and abrasive wear behaviour of boride coatings," Wear, vol. 256, no. 6, pp. 608-613, 2004.

[10] L. Yu, X. Chen, K. A. Khor, and G. Sundararajan, "FeB/Fe_2B phase transformation during SPS pack-boriding: boride layer growth kinetics," Acta Materialia, vol. 53, no. 8, pp. 2361-2368, 2005.

[11] H. Cimenoglu, E. Atar, and A. Motallebzadeh, "High temperature tribological behaviour of borided surfaces based on the phase structure of the boride layer," Wear, vol. 309, no. 1-2, pp. 152-158, 2014.

[12] E. Atık, U. Yunker, and C. Merıç, "The effects of conventional heat treatment and boronizing on abrasive wear and corrosion of SAE 1010, SAE 1040, D2 and 304 steels," Tribology International, vol. 36, no. 3, pp. 155-161, 2003.

[13] A. K. Sinha, "Boriding(Boronizing)," ASM International, ASM Handbook., vol. 4, pp. 437-447, 1991.

[14] N. Maragoudakis, G. Stergioudis, H. Omar, E. Pavlidou, and D. Tsipas, "Boro-nitriding of steel US 37-1," Materials Letters, vol. 57, no. 4, pp. 949-952, 2002.

[15] Y. Kar, N. Şen, and A. Demirbaş, "Boron minerals in Turkey, their application areas and importance for the country's economy," Minerals & Energy-Raw Materials Report, vol. 20, no. 3-4, pp. 2-10, 2006.

[16] H. B. Özerkan, "Simultaneous machining and surface alloying of AISI 1040 steel by electrical discharge machining with boron oxide powders," Journal of Mechanical Science and Technology, vol. 32, no. 9, pp. 4357-4364, 2018.

[17] R. I. Stephens, A. Fatemi, R. R. Stephens, and H. O. Fuchs, Metal fatigue in engineering. John Wiley & Sons, 2000.

[18] Y. Murakami, "Metal Fatigue: Effects of Small Defects and Nonmetallic Inclusions," Elsevier Science Ltd. UK," 2002.

[19] R. Pereira, F. Mariani, A. Neto, G. Totten, and L. Casteletti, "Characterization of layers produced by boriding and boriding-PVD on AISI D2 tool steel," Materials Performance and Characterization, vol. 5, no. 4, pp. 406-413, 2016.

[20] I. Ozbek and C. Bindal, "Mechanical properties of boronized AISI W4 steel," Surface and Coatings Technology, vol. 154, no. 1, pp. 14-20, 2002.

[21] M. Kul, I. Danacı, Ş. Gezer, and B. Karaca, "Effect of boronizing composition on hardness of boronized AISI 1045 steel," Materials Letters, vol. 279, p. 128510, 2020.

[22] A. A. Joshi and S. S. Hosmani, "Pack-boronizing of AISI 4140 steel: boronizing mechanism and the role of container design," Materials and Manufacturing Processes, vol. 29, no. 9, pp. 1062-1072, 2014.

[23] S. Şahin, "Effects of boronizing process on the surface roughness and dimensions of AISI 1020, AISI 1040 and AISI 2714," Journal of materials processing technology, vol. 209, no. 4, pp. 1736-1741, 2009.

[24] İ. Türkmen and E. Yalamaç, "Effect of Alternative Boronizing Mixtures on Boride Layer and Tribological Behaviour of Boronized SAE 1020 Steel," Metals and Materials International, pp. 1-15, 2021.

[25] F. Fernandes, L. Casteletti, S. Heck, and G. Totten, Wear evaluation of pack boronized AISI 1060 steel. ASTM International, 2013.

[26] K. Kasiviswanathan, K. Sudheer, and J. He, "Quantification of prediction uncertainty in artificial neural network models," in Artificial neural network modelling: Springer, 2016, pp. 145-159.

[27] R. Hristev, "The ANN book," ed: Edition, 1998.